Ballistic impact behavior of foam core sandwich structures: Formulation

N.K. Naik*, Ch.Veera Sesha Kumar
Indian Institute of Technology Bombay, Department of Aerospace Engineering
Powai, Mumbai 400 076, India

ABSTRACT

An analytical method based on the energy balance and wave propagation approach was developed for a sandwich panel subjected to a ballistic impact. Possible energy absorbing mechanisms in the complete perforation of a sandwich panel involve tensile fiber stretching and damage, matrix delamination and fracture, core compression and crushing, plugging, delamination between the core and bottom face sheet and friction. The complete perforation of the sandwich panel was modeled as 3-stage process that describes perforation of the top face sheet, complete densification of foam core, and perforation of the bottom face sheet sequentially. An experimental study was carried out to compare ballistic impact performance of foam core sandwich panel with composite face sheets to a plain composite laminate having same areal density.

Key words: Ballistic impact, Sandwich structure, Ballistic limit, Energy absorbing mechanism

1. INTRODUCTION

An essential requirement of high strength, high stiffness and lightweight materials has significantly increased the use of composites over past few decades in high performance applications. Composite sandwich panels are being used extensively in aerospace, marine, transportation and many other industries because of their exceptionally high flexural stiffness-to-weight ratio compared to other architectures. In many applications, composite sandwich structures may be subjected to localized projectile impact. Impact loads can be broadly classified into three categories: low velocity impact, high velocity impact and hyper velocity impact. The energy transfer between projectile and target, energy dissipation and damage propagation mechanisms vary significantly with the velocity of the projectile. A low-mass high velocity impact caused by a propelling source is generally referred to as ballistic impact. The applications involving survivability of personnel and equipments against penetration by high velocity projectiles are of significant importance and demand complete understanding of the perforation process of the composite sandwich structures subjected to ballistic impacts. Considering the importance, significant amount of work has been done on composite sandwich panels subjected to projectile impact at high velocities. Determination of the ballistic limit for a given sandwich structure was the prime objective of the past research. Although most of the research has been experimental, very few analytical solutions have been proposed. The analytical studies available did not consider all the energy absorbing mechanisms and are not completely based on energy balance and the wave propagation approach [1-5]. So there is need to develop an appropriate method to describe the perforation process in sandwich structures subjected to ballistic impacts. The main objective of this study is to develop an analytical method based on the wave propagation and energy balance approach for a sandwich panel subjected to ballistic impact.

2. BALLISTIC IMPACT PROCESS

Before starting mathematical formulation, it is highly essential to understand/anticipate what exactly happens in the material/structure during the penetration/perforation process. The complete perforation process can be divided into three stages that describe perforation of the top face sheet, complete densification of foam core, and perforation of the bottom face sheet sequentially. A sandwich panel as shown in Fig. 1(a) is impacted by a projectile with an incident velocity of V_o. The transverse impact on the target by the projectile generates through-the thickness compressive and shear waves along the thickness direction and tensile and shear waves along the radial direction.

* nknaik@aero.iitb.ac.in; Tel.: +91 22 2576 7114; fax: +91 22 2572 2602.

NOMENCLATURE

C_c	wave propagation velocity in the core
C_{fs}	wave propagation velocity in the face sheet
d	projectile diameter
d_{ci}	deceleration of the projectile during *i*th time interval
E_{CCi}	energy absorbed by core compression till time t_i
E_{CSPi}	energy absorbed by core shear plugging till time t_i
E_{Di}	energy absorbed by deformation of top face sheet secondary yarns till time t_i
E_{DDi}	energy dissipated by the core damping till time t_i
E_{D2i}	energy absorbed by deformation of bottom face sheet secondary yarns till time t_i
E_{DLi}	energy absorbed by delamination in top face sheet till time t_i
E_{DL2i}	energy absorbed by delamination between core and bottom face sheet till time t_i
E_{Fi}	energy absorbed by friction till time t_i
E_{FCi}	kinetic energy of the moving cone of top face sheet at time t_i
E_{MCi}	energy absorbed by matrix cracking in top face sheet till time t_i
E_{mt}	energy absorbed by matrix cracking per unit volume
E_{SPi}	energy absorbed by shear plugging of top face sheet till time t_i
E_{TFi}	energy absorbed by tensile failure of top face sheet primary yarns till time t_i
E_{TF2i}	energy absorbed by tensile failure of bottom face sheet primary yarns till time t_i
F_i	contact force during *i*th time interval
H_{Li}	distance travelled the compression wave through the thickness till time t_i
H_{Si}	distance travelled the shear wave through the thickness till time t_i
KE_{p0}	initial kinetic energy of the projectile
KE_{pi}	kinetic energy of the projectile at time t_i
L	length of the projectile
L_{Li}	radial distance reached by the longitudinal wave at time t_i
L_{Si}	radial distance reached by the shear wave at time t_i
M_{FCi}	mass of the face sheet cone at time t_i
m_p	mass of the projectile
r	impedance ratio
t_c	contact duration
t_1	thickness of the top face sheet
t_2	thickness of the bottom face sheet
t_c	thickness of the foam core
t_i	*i*th instant of time
V_i	projectile velocity at time t_i
V_{50}	ballistic limit velocity
V_0	incident impact velocity
V_R	residual velocity
z_i	depth of the cone at time t_i, distance travelled by projectile at time t_i
σ	stress
σ_I	incident stress
σ_R	reflected stress
σ_T	transmitted stress
ρ_c	density of core
ρ_{fs}	density of face sheet
Δt	duration of time interval

2.1 Stage 1

At any time instant t_i, the distance travelled the compression and shear waves through the thickness are represented by the H_{Li} and H_{Si} and radial distance reached by longitudinal and shear waves are represented by the L_{Li} and L_{Si} respectively as shown in Fig. 1(b).

Wave transmission, reflection and reverberation: When the compressive wave reaches the back face of the top face sheet, the wave encounters the boundary which is the interface between the face sheet and foam core. Because of the difference in impedance between face sheet and foam, the wave is partially transmitted and partially reflected. Since the impedance of the face sheet is much greater than the impedance of the foam, the impedance ratio would be very much lower. The transmission and reflection of a wave at a boundary depends on the impedance ratio.

The impedance ratio, $$r = \frac{\rho_c C_c}{\rho_{fs} C_{fs}} \tag{1}$$

The transmitted stress, $$\sigma_T = \frac{2r}{1+r}\sigma_I \tag{2}$$

The reflected stress, $$\sigma_R = -\frac{1-r}{1+r}\sigma_I \tag{3}$$

For a polymer foam core material (Divinycell HT) having density of 80 kg/m^3 and compressive modulus of 0.1 GPa, the impedance is 89.44 x 10^3 kg/m^2-sec. For a GFRP material having density of 1800 kg/m^3 and compressive modulus of 40 GPa, the impedance is 8.48 x 10^6 kg/m^2-sec. For the given impedance ratio of 0.01, it is interesting to note that, only 2% of the wave strength gets transmitted in to the core and 98% of the wave gets reflected as tensile wave. This reflected wave reaches the front face, encounters free boundary and reflects back as compressive wave again. So, this wave reverberates between the front and back face of top face sheet as compressive and tensile wave and transmits 2% every time into the core.

As the lateral wave propagates, the top face sheet undergoes local indentation upon the impact. The face sheet supported on the foam core behaves as a membrane resting on elastic-plastic foundation. The bonding between the top face sheet and the foam core transmits shear forces from the core to the face sheet. As the face sheet undergoes local indentation, the foam core experiences crushing in the region directly under the projectile. In the region surrounding the projectile and up to the surface radius of the lateral deformation, the foam core experiences both crushing and shear under the face sheet. The region beyond the surface radius of the lateral deformation is not affected yet by the moving wave at that particular time instant.

Top face sheet failure: When the shear wave reaches the backface of the top face sheet, the top face sheet might fail in shear if the shear force resulting from the impact exceeds the shear strength of the top face sheet material. If not, the top face sheet behaves as a membrane resting on the elastic-plastic foundation. The transverse wave in the top face sheet produces lateral deformation and tensile strain in the top face sheet. The top face sheet fails whenever the induced tensile stress exceeds the failure stress. Whether the top face sheet fails in tension or shear, depends on the material. Generally, the carbon fiber composites fail in shear plugging and glass fiber composites fail under tension since they exhibit much higher failure strains at higher strain rates. Appropriate failure theories need to be used to predict the failure of the top face sheet. The first ends when the top face sheet is completely perforated.

2.2 Stage 2

When the compressive wave reaches the front face of the bottom face sheet, the compressive wave again encounters another boundary which is the interface between the foam core and the bottom face sheet. The wave is again partially transmitted into the bottom face sheet and partially reflected back into the core because of the difference in impedance between face sheet and foam. The impedance of the foam is much lower than the impedance of the face sheet. For an impedance ratio of around 100, almost double the strength of compressive wave strength gets transmitted in to the bottom face sheet and 98% of the wave gets reflected back into the core as compressive wave.

Bonding failure: If the strength of the compressive wave reaching the bottom face sheet exceeds the adhesive strength, the delamination takes place between the foam core and the bottom face sheet. Once the delamination occurs, the bottom face sheet deforms independently from the core.
When the compressive wave reaches the back face of the bottom face sheet, it encounters free surface and gets reflected back in the skin completely as a tensile wave. As the projectile penetrates further, the core densifies further and the delamination size increases further.

Core failure: When the shear wave reaches the bottom face sheet, the core might fail in shear completely along thickness direction. The second stage ends when the core densifies completely and forms a plug as shown in Fig. 1(c).

2.3 Stage 3

The projectile motion along with the plug increases the delamination size continuously. The bottom face sheet ruptures under tension when the induced stress exceeds failure stress of the face sheet material. The tensile failure of the bottom face sheet forms petals as shown in Fig. 1(d). The plug along with the projectile could eject out with some residual velocity. If the projectile is propelled at ballistic limit, the residual velocity of the projectile becomes zero when plug reaches the back face of the bottom face sheet.

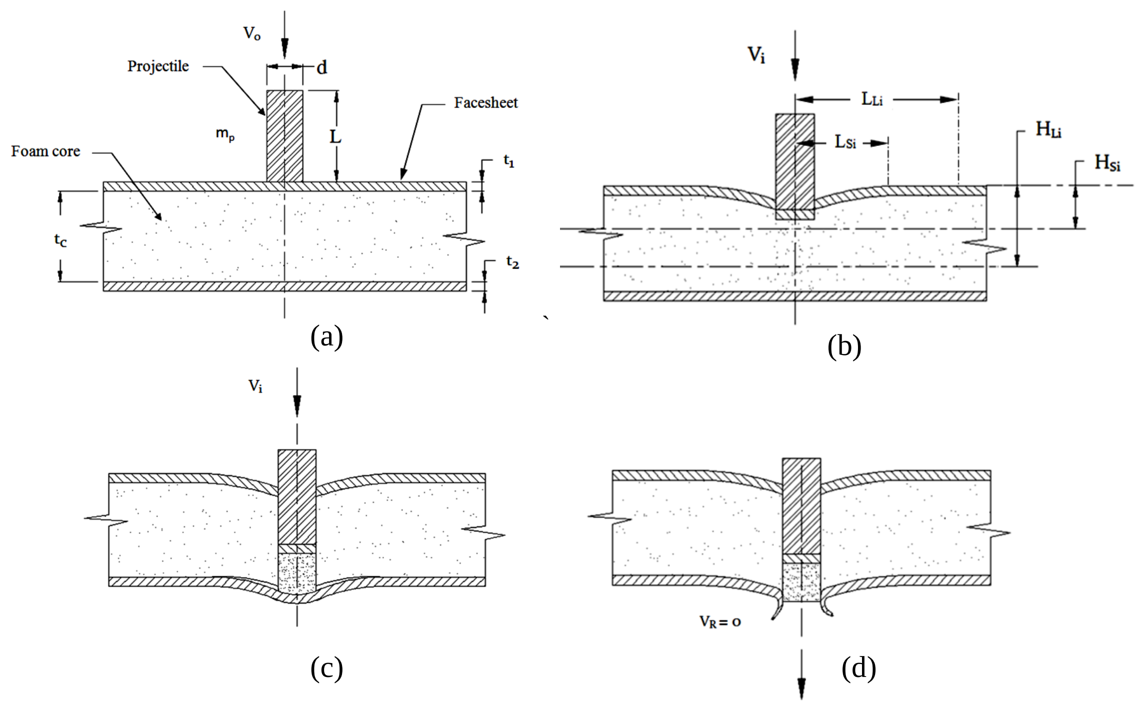

Fig. 1 Perforation process through sandwich structure

3. ANALYTICAL FORMULATION

The main objective of the analytical formulation is to predict the ballistic limit, contact duration, and damage size. The formulation is based on wave propagation approach and the energy balance between the projectile and the target material. The analysis requires the geometrical and mechanical characteristics of the target material and projectile as the input parameters.

3.1 Assumptions

1. The thickness of the face sheet is much lower than the core thickness, $h < H$.
2. The top face sheet deflection and perforation takes place during the foam core crushing. The bottom face sheet is undeformed during top face sheet indentation.
3. Projectile impact is normal to the surface of the target.
4. Projectile is considered to be rigid and remains un-deformed during the ballistic impact.
5. During any time interval, the projectile motion is uniform and the velocity of the projectile remains constant
6. Energy absorption due to primary yarn/fiber breakage and deformation of the secondary yarns are treated independently.
7. Longitudinal and transverse wave velocities are the same in all the layers.
8. The projectile is cylindrical with a flat end.

3.2 Energy balance

As the projectile impacts the target, the energy lost by the projectile is absorbed by the target material through different energy absorbing mechanisms. The perforation of a face sheet involve various damage and energy absorbing mechanisms like face sheet cone formation, shear plugging, tension in primary yarns, deformation of secondary yarns, delamination, matrix cracking and friction during penetration [6]. In addition, the foam core absorbs some energy in the form of core compression, crushing, shear plugging and damping. The delamination between the core and bottom face sheet also absorbs considerable energy. The load duration is divided into small time intervals and the velocity of the projectile at the end of any *i*th time interval can be expressed from the energy balance. Initial kinetic energy of the projectile can be expressed as the summation of residual kinetic energy of the projectile and the energy absorbed by all mechanisms.

$$KE_{p0} = KE_{pi} + \left\{E_{FCi} + E_{SP(i-1)} + E_{TF(i-1)} + E_{D(i-1)} + E_{DL(i-1)} + E_{MC(i-1)}\right\} + \left\{E_{CC(i-1)} + E_{CSP(i-1)} + E_{DD(i-1)}\right\} + \left\{E_{DL2(i-1)} + E_{TF2(i-1)} + E_{D2(i-1)}\right\} + E_{F(i-1)} \tag{4}$$

$$\frac{1}{2} m_p V_0^2 - E_{i-1} = \frac{1}{2}(m_p + M_{FCi}) V_i^2 \tag{5}$$

$$E_{i-1} = \left\{E_{SP(i-1)} + E_{TF(i-1)} + E_{D(i-1)} + E_{DL(i-1)} + E_{MC(i-1)}\right\} + \left\{E_{cc(i-1)} + E_{CSP(i-1)}\right\} + \left\{E_{DL2(i-1)} + E_{TF2(i-1)} + E_{D2(i-1)}\right\} + E_{F(i-1)} \tag{6}$$

3.3 Projectile velocity

The velocity of the projectile at the end of *i*th time interval can be obtained from Eq. (4-6) and is given by

$$V_i = \sqrt{\frac{\frac{1}{2} m_p V_0^2 - E_{i-1}}{\frac{1}{2}(m_p + M_{FCi})}} \tag{7}$$

The projectile velocity at the end of first interval is derived by equating the rate of change of momentum of the moving mass to the force acting on the projectile [7]. Once the velocity is obtained for the first interval, the energy absorbed by different energy-absorbing mechanisms during first time interval is calculated. The velocity of the projectile for the next time interval can be calculated using Eq. (7). From the velocity at end of each time interval, various parameters such as displacement of projectile, strain, contact force, and energy absorbed by different mechanisms are calculated for the given time interval. This procedure continues till either the sandwich panel is completely perforated or the velocity of the projectile becomes zero within the sandwich panel. The ballistic limit is found by equating the residual velocity at the projectile exit to zero and by calculating corresponding initial velocity through iterative process.

3.4 Contact force

The projectile continuously decelerates as the target material absorbs some energy in every time interval. The contact force can be expressed as the product of mass and deceleration of the projectile. The deceleration of the projectile during the time interval is given by

$$dc_i = \frac{V_{i-1} - V_i}{\Delta t} \tag{8}$$

The force resisting the projectile motion,

$$F_i = m_p dc_i \tag{9}$$

3.5 Distance traveled by the projectile / cone depth

The distance traveled by the projectile during *i*th time interval is obtained as

$$\Delta z_i = V_{i-1}\Delta t - \frac{1}{2} dc_i (\Delta t)^2 \tag{10}$$

Distance travelled by the projectile z_i up to *i*th time interval is given by

$$z_i = \sum_{n=0}^{n=i} \Delta z_n \tag{11}$$

3.6 Contact duration

The penetration or perforation process starts when the projectile touches the front face of the top face sheet and ends when sandwich completely fails or when the velocity of the projectile becomes zero. Total time taken by the projectile in the penetration or perforation process is called as contact duration and is given by

$$t_c = n\Delta t \tag{12}$$

3.7 Damage size

The magnitude of strain varies around the impacted zone because of the stress wave attenuation. The strain decreases along the radius of the damage zone from a maximum value at the point of impact. Whenever the strain at the point of impact exceeds the ultimate strain, the fiber breakage takes place resulting in face sheet failure. Clearly visible damage would be seen in the region, around the point of impact, in which the strain exceeds the damage threshold strain. The radius of damage zone can be obtained from the strain profiles along the radius at different time instants.

4. SOLUTION PROCEDURE

The velocity of the projectile at the end of *i*th time interval can be determined from the energy balance as given by Eq. (7). During the initial part of stage 1, the compressive and shear waves do not reach the bottom face sheet and hence all the energy terms associated with the bottom face sheet in Eq. (4) remain zero. Once the top face sheet is perforated, stage 1 ends and all the energy terms associated with the top face sheet vanish. After the foam core is completely sheared and crushed, stage 2 ends and all the energy terms associated with the top face sheet and the foam core vanish. Energy is absorbed by the delamination between the foam core and bottom face sheet and the deformation of the bottom face sheet. Finally, when the bottom face sheet ruptures under tension, all the energy terms associated with the target material vanish except the residual kinetic energy of the projectile from which the exit velocity of the projectile can be calculated.

The analytical method requires complete geometrical and material data related to the projectile, face sheet and the foam. The analysis part involves stepwise analysis of top face sheet, core and bottom face sheet. Each step in turn involves solution of simultaneous equations and calculation of projectile velocity. From the velocity at end of each time interval, various parameters such as displacement of projectile, strain, contact force, and energy absorbed by different mechanisms are calculated for the given time interval. This procedure continues till either the sandwich panel is completely perforated or the velocity of the projectile becomes zero within the sandwich panel. The ballistic limit is found by equating the residual velocity at the projectile exit to zero and by calculating the initial velocity through iterative process

5. EXPERIMENTAL CHARACTERIZATION OF BALLISTIC IMPACT BEHAVIOR

Several experimental studies have been carried out on the ballistic impact performance of the sandwich structures and reported in the literature [8-15]. Determination of the ballistic limit for the given composite sandwich panel was the prime objective of the past research. Every experiment in the literature has been carried out on specific target material and sandwich configuration impacted by a projectile of specific size and shape. But, none of the study reported in the literature compares ballistic performance of a composite sandwich panel to a plain composite laminate having same areal density. So, an experimental study was carried out to compare ballistic impact performance of a foam core sandwich panel with E-glass/epoxy face sheets to a plain E-glass/epoxy composite laminate having same areal density.

5.1 Test specimen

Plain composite laminates used for the ballistic impact testing experiments were fabricated using E-glass plain weave fabric and epoxy LY 556 with hardener HY 951. 150 mm x 150 mm specimens of 4 mm thickness were cut from the cured laminate for experimental testing. Fiber volume fraction of laminate was 0.4.

Foam core sandwich panels were fabricated in such a way that the areal density of sandwich panel and the plain composite laminate were the same. Face sheet thickness was appropriately reduced to account for the weight of the foam. Face sheets were fabricated separately and bonded to the foam core of 12 mm thickness on either side using epoxy LY 556 and hardener HY 951. Volume fraction for the face sheet laminates was also 0.4.

5.2 Experimental observations

From the experimental results, the ballistic limit velocity for the plain composite laminate of 4 mm thickness was found to be in the range of 159 m/s to 163 m/s. For the given projectile size and shape, the velocity at which the projectile is expected to perforate the target at 50 % probability, the ballistic limit is typically denoted as the V_{50} value. Hence the ballistic limit, V_{50} is 161 m/s for the composite laminate of 4 mm thickness. For the sandwich specimens having same areal density, the ballistic limit velocity was found to be in the range of 182 m/s to 191 m/s. Hence V_{50} for sandwich structure is 186.5 m/s. The test results reveal that the ballistic limit for sandwich structure is significantly higher than that of plain composite laminate with the same areal density. The increase in ballistic limit and the energy absorbed are 16 % and 35 % respectively.

6. CONCLUDING REMARKS

An analytical method based on the energy balance and wave propagation approach has been proposed to predict the ballistic impact performance of a foam core sandwich composite structure. The complete perforation of the sandwich panel was modeled as 3-stage process that describe perforation of the top face sheet, complete densification of foam core, and perforation of the bottom face sheet sequentially. Possible energy absorbing mechanisms in the complete perforation of a sandwich panel involve face sheet cone formation, tensile fiber stretching and fracture, shear plugging, matrix cracking and delamination, core compression, crushing and plugging, delamination between the core and facings and friction. An experiment carried out on a foam core sandwich panel with E-glass/epoxy face sheets exhibited higher ballistic limit compared to a plain E-glass/epoxy composite laminate having same areal weight. The preliminary results based on the analytical method presented also show that the ballistic limit velocity for the foam core sandwich structure is significantly higher than that for composite laminate with the same areal density.

REFERENCES

[1] Skvortsov, V., Kepler, J. and Bozhevolnaya, E., “Energy partition for ballistic penetration of sandwich panels”, International Journal of Impact Engineering, 28(7), 697-716 (2003).

[2] Hoo Fatt, M.S. and Park, K.S., “Perforation of honeycomb sandwich plates by projectiles”, Composites Part A: Applied Science and Manufacturing, 31(8), 889-899 (2008).

[3] Fatt, M.S.H. and Sirivolu, D., “Impact perforation of sandwich panels with Coremat”, International Journal of Crashworthiness, 14(1), 37-47 (2009).

[4] Chunfu Lin and Hoo Fatt, M.S., “Perforation of composite plates and sandwich panels under quasi-static and projectile loading”, Journal of Composite Materials, 40(20), 1801-1840 (2006).

[5] Fatt, M.S.H. and Sirivolu, D.A., “wave propagation model for the high velocity impact response of a composite sandwich panel”, International Journal of Impact Engineering, 37(2), 117-130 (2010).

[6] Naik, N. K., Shrirao, P. and Reddy, B.C.K., "Ballistic impact behaviour of woven fabric composites: Formulation”, International Journal of Impact Engineering, 32(9), 1521-1552 (2006).

[7] Naik, N. K. and Doshi, A.V., “Ballistic impact behavior of thick composites: analytical formulation”, AIAA Journal, 43(7), 1525-1536 (2005).

[8] Alavi Nia, A., Razavi, S.B. and Majzoobi, G.H., “Ballistic limit determination of aluminum honeycombs - experimental study”, Materials Science & Engineering: A, 488(1-2), 273-280 (2008).

[9] Ryan, S., Schaefer, F., Destefanis, R. and Lambert, M., “A ballistic limit equation for hypervelocity impacts on composite honeycomb sandwich panel satellite structures”, Advances in Space Research, 41(7) 1152-1166 (2008).

[10] Zhou, D.W. and Stronge, W.J., “Ballistic limit for oblique impact of thin sandwich panels and spaced plates”, International Journal of Impact Engineering, 35(11), 1339-1354 (2008).

[11] Yungwirth, C.J., Radford, D.D., Aronson, M. and Wadley, H.N.G., “Experiment assessment of the ballistic response of composite pyramidal lattice truss structures”, Composites Part B: Engineering, 39(3), 556-569 (2008).

[12] Hou, W., Zhu, F., Lu, G. and Fang, D., “Ballistic impact experiments of metallic sandwich panels with aluminium foam core”, International Journal of Impact Engineering, 37(10), 1045-1055(2010).

[13] Destefanis, R., Schafer, F., Lambert, M. and Faraud, M., “Selecting enhanced space debris shields for manned spacecraft.” International Journal of Impact Engineering 33(1-12), 219-230 (2006).

[14] Bull, P.H. and Kepler, J., “Sensitivity of structurally loaded sandwich panels to localized ballistic penetration”, Composites Science and Technology, 69(6), 696-703 (2009).

[15] Reyes Villanueva, G. and Cantwell, W.J., “The high velocity impact response of composite and FML-reinforced sandwich structures”, Composites Science and Technology, 64(1), 35-54 (2004).